Computational Mechanics 28 (2002) 47–54 © Springer-Verlag 2002
DOI 10.1007/s00466-001-0268-9

A boundary point interpolation method for stress analysis of solids

Y. T. Gu, G. R. Liu

Abstract A boundary point interpolation method (BPIM) is proposed for solving boundary value problems of solid mechanics. In the BPIM, the boundary of a problem domain is represented by properly scattered nodes. The boundary integral equation (BIE) for 2-D elastostatics has been discretized using point interpolants based only on a group of arbitrarily distributed boundary points. In the present BPIM formulation, the shape functions constructed using polynomial basis function in a curvilinear coordinate possess Dirac delta function property. The boundary conditions can be implemented with ease as in the conventional boundary element method (BEM). The BPIM for 2-D elastostatics has been coded in FORTRAN, and used to obtain numerical results for stress analysis of two-dimensional solids.

1 Introduction

In application of traditional finite element method (FEM), mesh generation can be a very time-consuming and burdensome task especially when a re-meshing is required in the computing process. Therefore, element free or meshless methods have been proposed in recent years and achieved remarkable progress. Nayroles et al. (1992) proposed a technique called diffuse element method (DEM). Liu et al. (1995) developed a reproducing kernel particle method (RKPM). Atluri and Zhu (1998) and Atluri et al. (1999) proposed a meshless local Petrov-Galerkin (MLPG) method. Belytschko et al. (1994) refined and modified the DEM to formulate the so-called element-free Galerkin (EFG) method.

The EFG method has been further advanced significantly recent years, and applied to a variety of problems of mechanics. However, there exist some disadvantages in using EFG. Strategies have been developed for the alleviation of the drawbacks of EFG (Zhu and Atluri, 1998; Liu, 1999; Liu and Yang, 1998). A meshless method, called point interpolation method (PIM), has been proposed (Liu and Gu, 2001; Wang et al., 2001). The shape functions in PIM constructed using polynomial interpolation possess delta property. Techniques of coupling EFG with other established numerical methods have also been proposed, such as coupled EFG/finite element (FE) methods (Belytschko and Organ, 1995; Hegen, 1996), the coupled EFG/boundary element (BE) method (Gu and Liu, 2001) and the coupled EFG/hybrid BE method (Liu and Gu, 2000).

The boundary element method (BEM) is a numerical technique based on boundary integral equation (BIE), which has been developed since 1960's. For many problems, the BEM is undoubtedly superior to the 'domain' type methods, such as FEM. BEM has a well-known dimensionality advantage for linear problems. For example, only 2-D bounding surface of a 3-D body needs to be discretized. The idea of meshless has also been used in BIE, such as the local boundary integral equation (LBIE) method (Zhu et al., 1998) and the boundary node method (BNM) (Mukherjee and Mukherjee, 1997; Kothnur et al., 1999). The moving least squares (MLS) approximation is combined with BIE to propose a boundary type meshless method called boundary node method (BNM). In BNM, the surface of problem domain is discretized by properly scattered nodes. The BNM has been applied to 3-dimesional problems in potential theory and elasto-statics (Chati and Mukherjee, 2000; Chati et al., 1999). Very good results are obtained in these problems. However, because the shape functions based on MLS interpolants lack delta function property, it is difficult to accurately satisfy the boundary condition in BNM. This problem becomes even more serious in BNM because a large number of boundary conditions need be satisfied. The method used by Kothnur et al. (1999) to impose boundary conditions doubles the number of system equations, making BNM computationally much more expensive than the conventional BEM.

A boundary point interpolation method (BPIM) is proposed in this paper. The polynomial interpolants based on scattered nodes are used to construct the shape functions. The BPIM employs the point interpolation technique in the BIE, based on the similar idea of the BNM. Because the shape functions possess delta function property, BPIM overcomes the shortcomings of BNM. The imposition of boundary conditions in BPIM is as easy as in the traditional BEM. In addition, the rigid body movement can also be utilized to avoid some singular integrals.

A program of BPIM for 2-D elastostatics is developed in FORTRAN, and several numerical examples are presented to demonstrate the validity and efficiency of the BPIM. A BNM program and a conventional BEM program are also developed. A comparison study is carried out using BPIM, BNM, conventional BEM and analytical methods.

Received 10 January 2000

Y. T. Gu, G. R. Liu (✉)
Department of Mechanical Engineering,
National University of Singapore,
10 Kent Ridge Crescent, Singapore 119260
e-mail: engp8973@nus.edu.sg; mpeliugr@nus.edu.sg

2
Point interpolation

The point interpolants in BPIM are constructed on the 1-D bounding curve Γ of 2-D domain Ω, using a set of discrete nodes on Γ. As in the conventional BEM formulation, the displacement and traction can be constructed independently using point interpolation. The point interpolation for displacement $u(s)$ and traction $t(s)$ at a point s on the boundary Γ from the surrounding nodes uses polynomials

$$u(s) = \sum_{i=1}^{n} p_i(s) a_i = \mathbf{p}^{\mathrm{T}}(s)\mathbf{a} \tag{1a}$$

$$t(s) = \sum_{i=1}^{n} p_i(s) b_i = \mathbf{p}^{\mathrm{T}}(s)\mathbf{b} \tag{1b}$$

where s is a curvilinear co-ordinate (the arc length for 2-D problem) on Γ, n is the number of nodes in the neighborhood of a point s, $p_i(s)$ is a basis function of a complete polynomial with $p_1 = 1$ and $p_i = s^{i-1}$, a_i and b_i are the coefficients. In matrix form, we have

$$\mathbf{a}^{\mathrm{T}} = [a_1, a_2, a_3, \ldots, a_n] \tag{2a}$$

$$\mathbf{b}^{\mathrm{T}} = [b_1, b_2, b_3, \ldots, b_n] \tag{2b}$$

$$\mathbf{p}^{\mathrm{T}}(s) = [1, s, s^2, s^3, s^4, \ldots, s^{n-1}] \tag{3}$$

The coefficients a_i and b_i in Eq. (1) can be determined by enforcing Eq. (1) to be satisfied at the n nodes surrounding the point s. Equation (1) can be then written in the following matrix form.

$$\mathbf{u}_n = \mathbf{P}_Q \mathbf{a} \tag{4a}$$

$$\mathbf{t}_n = \mathbf{P}_Q \mathbf{b} \tag{4b}$$

where $\mathbf{u}_n$ and $\mathbf{t}_n$ are the vectors of nodal displacement and traction, given by

$$\mathbf{u}_n = [u_1, u_2, u_3, \ldots, u_n]^{\mathrm{T}} \tag{5a}$$

$$\mathbf{t}_n = [t_1, t_2, t_3, \ldots, t_n]^{\mathrm{T}} \tag{5b}$$

and $\mathbf{P}_Q$ is a matrix of

$$\mathbf{P}_Q^{\mathrm{T}} = [\mathbf{p}(s_1), \mathbf{p}(s_2), \mathbf{p}(s_3), \ldots, \mathbf{p}(s_n)] \tag{6}$$

Solving $\mathbf{a}$ and $\mathbf{b}$ from Eq. (4), and then substituting them into Eq. (1), we obtain

$$u(s) = \mathbf{\Phi}^{\mathrm{T}}(s)\mathbf{u}_n \tag{7a}$$

$$t(s) = \mathbf{\Phi}^{\mathrm{T}}(s)\mathbf{t}_n \tag{7b}$$

where the shape function $\mathbf{\Phi}(s)$ is defined by

$$\mathbf{\Phi}^{\mathrm{T}}(s) = \mathbf{p}^{\mathrm{T}}(s)\mathbf{P}_Q^{-1} = [\phi_1(s), \phi_2(s), \phi_3(s), \ldots, \phi_n(s)] \tag{8}$$

The shape function $\phi_i(s)$ obtained through above procedure satisfies

$$\phi_i(s = s_i) = 1 \quad i = 1, n \tag{9a}$$

$$\phi_j(s = s_i) = 0 \quad j \neq i \tag{9b}$$

$$\sum_{i=1}^{n} \phi_i(s) = 1 \tag{9c}$$

Therefore, the shape functions constructed have delta function property, and the boundary conditions can be easily imposed as in the traditional BEM.

The matrix $\mathbf{P}_Q$ is an $n \times n$ matrix. It needs to be invertible for the construction of the shape functions in Eq. (8). Utilization the curvilinear co-ordinate, the matrix $\mathbf{P}_Q$ is, in general, reversible for the 2-D problem (interpolation along a 1-D boundary). It is also desirable that $\mathbf{P}_Q$ be well conditioned in order to reduce the numerical errors (Chati and Mukherjee, 2000). It can be found that the condition number of the $\mathbf{P}_Q$ depends on the nodes in the influence domain of a sampling point. In general, the condition number of the $\mathbf{P}_Q$ will increase with the increase of the number of nodes, n, in the influence domain. Therefore the influence domain should be chosen to obtain a well conditioned $\mathbf{P}_Q$.

In order to define the influence domain for a point s_i, a curvilinear influence domain is used. The arc length of the curvilinear domain d_{mi} is computed by

$$d_{mi} = d_{\max} e_i \tag{10}$$

where $d_{\max}$ is a scaling parameter, e_i is a parameter of distance. If the nodes are uniformly distributed, e_i is the maximum distance between two nodes. In the case where the nodes are randomly distributed, e_i can be defined as a characteristic arc length of the integration zone that contains point s_i (Belytschko et al., 1994). The number of nodes, n, can be determined by counting all the nodes in the influence domain. It can be observed that choosing $d_{\max} = 2.0$–3.0 ($n = 3$–6) leads to acceptable results.

3
BPIM formulation

3.1
Discrete equations of BPIM

The well-known BIE formulation for 2-D linear elastostatics, presented by Brebbia (1978), is given by

$$c_i \mathbf{u}_i + \int_{\Gamma} \mathbf{u}\mathbf{t}^* \mathrm{d}\Gamma = \int_{\Gamma} \mathbf{t}\mathbf{u}^* \mathrm{d}\Gamma + \int_{\Omega} \mathbf{b}\mathbf{u}^* \mathrm{d}\Omega \tag{11}$$

where c_i is a coefficient depended on the geometrical shape of boundary. $\mathbf{b}$ is the body force vector, $\mathbf{u}^*$ and $\mathbf{t}^*$ are the fundamental solution for linear elastostatics. The fundamental solution (Brebbia et al., 1984) for 2-D plane strain problem is given by

$$u_{ij}^* = \frac{1}{8\pi G(1-\nu)} \left\{ (3 - 4\nu) \ln \frac{1}{r} \Delta_{ij} + r_{,i} r_{,j} \right\} \tag{12a}$$

$$t_{ij}^* = \frac{-1}{4\pi(1-\nu)r} \left\{ \frac{\partial r}{\partial n} [(1-2\nu)\Delta_{ij} + r_{,i} r_{,j}] - (1-2\nu)(r_{,i} n_{,j} - r_{,j} n_{,i}) \right\} \tag{12b}$$

where G is the shear modulus, ν is the Poisson's ratio, Δ is the Kronecker delta function, r is the distance between

a source point and a field point, n is the normal to the boundary, a comma designates a partial derivative with respect to the indicated spatial variable.

Substituting Eq. (7) into Eq. (11) yields the BPIM system equation

$$\mathbf{H}\mathbf{u}_n = \mathbf{G}\mathbf{t}_n + \mathbf{d} \tag{13}$$

where

$$\mathbf{H} = c_i + \int_\Gamma \mathbf{t}^* \mathbf{\Phi}^{\mathrm{T}} \mathrm{d}\Gamma \tag{14a}$$

$$\mathbf{G} = \int_\Gamma \mathbf{u}^* \mathbf{\Phi}^{\mathrm{T}} \mathrm{d}\Gamma \tag{14b}$$

$$\mathbf{d} = \int_\Omega \mathbf{b}\mathbf{u}^* \mathrm{d}\Omega \tag{14c}$$

3.2 Comparison between BPIM, BNM and BEM

A comparison between BPIM, BNM and BEM is summarized concisely in Table 1. It can be found that BPIM, BNM and BEM are all based on the boundary integral equation. The difference is in the means of implementation.

BPIM versus BEM

Both BPIM and BEM use the polynomial interpolants, in which the number of monomials used in the base functions, m, is the same as the number of nodes, n, utilized. Therefore, the interpolant functions possess the Dirac delta function properties. The boundary conditions can be implemented with ease.

However, the BPIM is a boundary type meshless method when the BEM is a boundary type method based on the mesh. As other meshless methods (e.g. EFG, BNM, MLPG), the interpolation procedure in the BPIM is based only on a group of arbitrary distributed nodes as above discussed. The interpolation procedure in the BEM is based on an element. As shown in Fig. 1, the interpolation at a sampling point in the BPIM is performed over the influence domain of the point, which may overlap with the influence domains of other sampling points. BEM defines the shape functions over pre-defined regions called elements, and there is no overlapping at all.

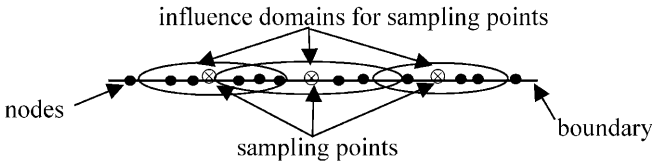

Fig. 1. The interpolation in BPIM

BPIM versus BNM

Both BPIM and BNM are boundary type meshless methods. The difference between these two methods comes from the different interpolants utilized. As above discussed, the BPIM uses passing nodes polynomial interpolants, in which the coefficients a and b in Eq. (1) are constant. The moving least squares (MLS) interpolants are used in the BNM, in which a and b are also functions of curvilinear co-ordinate s. Therefore, the shape function of BNM is more complicated than PIM. In addition, the shape function of BNM constructed using the MLS approximation lacks the delta function property. It takes extra effort to impose boundary conditions.

4 Implementation of BPIM

4.1 Singular integral

In order to obtain the integrals in Eq. (14), background integration cells that can be independent of the nodes are required. From Eq. (12), it is can be seen that the integrands in Eq. (14) consist of regular and singular functions. The regular functions in Eq. (14) can be evaluated using the usual Gaussian quadrature based on the integration cells. In Eq. (14b), the matrix $\mathbf{G}$ contains a log singular integral. This type of singular integral can be evaluated by log Gaussian quadrature as follows:

$$I = \int_0^1 \ln(1/x) f(x) \mathrm{d}x \cong \sum_{i=1}^{m} f(x_i) w_i \tag{15}$$

Table 1. Comparison between BPIM, BNM and BEM

	BPIM	BNM	BEM
Mesh	No	No	Yes
Interpolants	Polynomial	MLS	Polynomial
Interpolation area based on	Distributed nodes	Distributed nodes	Element
Number of basis m and interpolation nodes n	$m = n$	$m \neq n$	$m = n$
Overlapping of interpolation area	Overlapping	Overlapping	No overlapping
Shape function	Simple	Complicated	Simple
Delta property of shape function	Yes	No	Yes
Application of boundary conditions	Easy	Difficult	Easy
Number of system equations	$2N_B$	$4N_B$	$2N_B$

where the required points x_i and weights w_i are presented by Brebbia et al. (1984).

In matrix $\mathbf{H}$, c is a coefficient depended on the geometrical shape of the boundary, which is easy to be obtained for a smooth boundary. However, it is more complicated to obtain c for non-smooth boundaries. In addition, $\mathbf{H}$ contains $(1/r)$ type singular integral. Therefore, it can be a non-trivial task to directly evaluate the diagonal terms of $\mathbf{H}$. Note that shape functions of BPIM possess delta function property, therefore, the rigid body movement can be utilized in this work to obtain the diagonal terms of $\mathbf{H}$ (Brebbia et al., 1984).

4.2 Application of boundary conditions

There are two types of boundary conditions in BPIM

$$\mathbf{t} = \bar{\mathbf{t}} \quad \text{on the natural boundary } \Gamma_t \tag{16a}$$

$$\mathbf{u} = \bar{\mathbf{u}} \quad \text{on the essential boundary } \Gamma_u \tag{16b}$$

Because the shape functions of BPIM have delta property, the boundary conditions can be imposed in the same way as the traditional BEM. After applying the boundary condition, the system equation (13) has $2N_B$ equations and $2N_B$ unknowns for N_B boundary nodes. The system equation can be solved in a standard way to obtain the displacement and traction.

4.3 Handling of corners with traction discontinuities

In handling traction discontinuities in corners, special care should be taken. Double nodes and discontinuous elements at corners are used to overcome this problem in the traditional BEM. Because there are no elements used in BPIM, a simple method proposed here to solve this difficulty is by displacing the nodes from the corner. In addition, the influence domain for interpolation is truncated at the corner. The method is very easy to implement and is used in the following numerical examples. The simple method is proven to be very accurate.

5 Numerical examples

The BPIM is coded in FORTRAN. A detailed comparison study is carried out for a number of problems using the present BPIM, BNM, conventional BEM and analytic methods. The exponential weight function (Kothnur et al., 1999) is used in BNM analysis, i.e.

$$w_i(s) = \begin{cases} \dfrac{\mathrm{e}^{-(d_i/c)^{2k}} - \mathrm{e}^{-(d_{mi}/c)^{2k}}}{1-\mathrm{e}^{-(d_{mi}/c)^{2k}}} & d \le d_{mi} \\ 0 & d > d_{mi} \end{cases} \tag{17}$$

where d_i is the arc length, d_{mi} is the size of the support of the weight function w_i, k and c are constants. In this paper, $k = 1$ and $d_m/c = 0.75$ are used (Kothnur et al., 1999).

5.1 Cantilever beam

The BPIM is first applied to obtain the solution of a cantilever beam, which is shown in Fig. 2. A plane stress problem is considered. The elastic constants for the beam are: $E = 3.0 \times 10^7$, and $\nu = 0.3$. The length L and height D of beam are 48 and 12, respectively. The beam is subjected to a parabolic traction at the free end. The analytical solution is available and can be found in a textbook by Timoshenko and Goodier (1970).

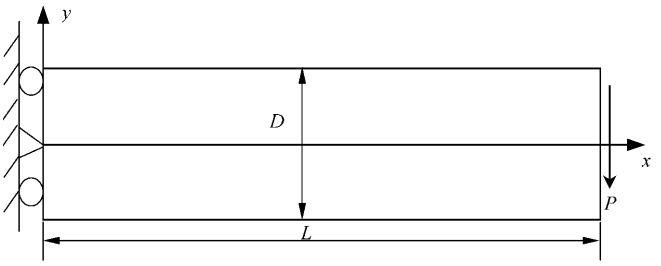

Fig. 2. Cantilever beam

For the detailed error analysis, we define the following norm as an error indicator using the shear stress, as the shear stress is much more critical than other stress components in the cantilever beam to reflect the accuracy.

$$e_t = \frac{1}{N}\sqrt{\sum_{i=1}^{N}(\tau_i - \bar{\tau}_i)^2 \Big/ \sum_{i=1}^{N}\bar{\tau}^2} \tag{18}$$

where N is the number of nodes investigated, τ is the shear stress obtained numerically, and $\bar{\tau}$ is the analytical shear stress.

A total of 120 uniform boundary nodes are used to discretize the boundary of the beam. One hundred twenty uniform integration cells are used to evaluate the integral of matrixes.

As above mentioned, the parameter $d_{\max}$ in Eq. (10) needs to be chosen such that a 'reasonable' number of nodes are included in the influence domain of an evaluation point. The results of e_t for different influence domains of an evaluation point are plotted in Fig. 3. In this analysis, the boundary is discretized by 40 uniformly distributed nodes. Forty integration background cells, uniformly spaced, are used. It is found that the accuracy of the results of BPIM changes a little with influence domain when the nodal density is fixed. A too small influence domain ($d_{\max} < 2.0$) and a too big influence domain ($d_{\max} > 4.0$) lead big errors. The bad accuracy of a too small influence domain is because that there are not enough nodes to perform interpolation for the field variable. In the contrary, a too big influence domain will increase the numerical error of integrations because the order of the interpolants is too high. Although the choosing of the

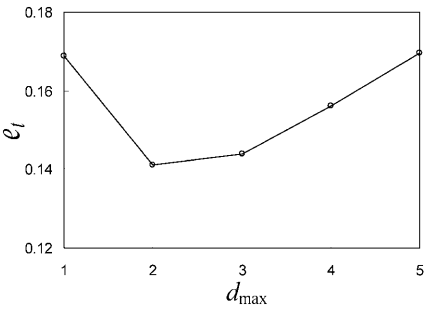

Fig. 3. Influence of parameter $d_{\max}$ of the influence domain

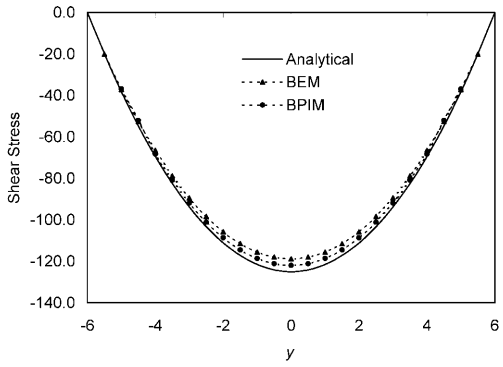

Fig. 4. Shear stress τ_{xy} at the section $x = L/2$ of the beam

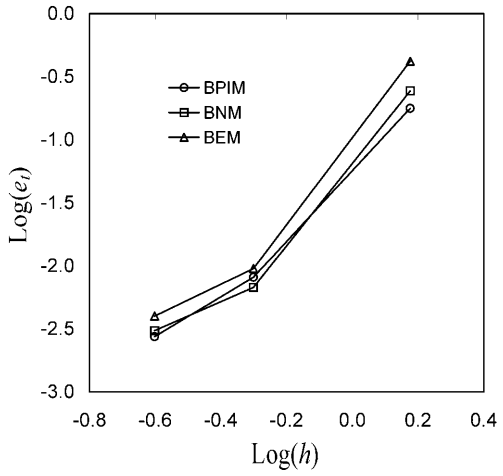

Fig. 5. Convergence in e_t norm of error

influence domain may also depend a little on the type of the problem, it is found that $d_{\max} = 2.0$–3.0 works for most of the problems investigated in this paper. Therefore, $d_{\max} = 2.0$ is used for the influence domains of all evaluation points in the boundary. By counting all the nodes in the influence domain, 3–6 nodes are usually used in the interpolation for all evaluation points.

Figure 4 illustrates the comparison between the shear stress calculated analytically and by the BPIM at the section of $x = L/2$. The plot shows a good agreement between the analytical and numerical results. The conventional linear BEM results of this problem are also shown in the same figure for comparison. The density of the nodes in the BEM and BPIM is exactly the same. It is clearly shown that the BPIM results are more accurate than BEM results. This is because the BPIM uses more nodes for the interpolation of the displacement and traction. Therefore, the order of the interpolant in the BPIM is higher than that of the conventional linear BEM.

The convergence for the shear stresses at the section of $x = L/2$ with mesh refinement is shown in Fig. 5, where h is a characteristic length equivalent to the maximum element size in the BEM. Three kinds of nodal arrangement of 40, 240 and 480 uniform boundary nodes are used. It is observed that the convergence of the BPIM is very good. The convergences of BNM and the conventional linear BEM are also shown in the same figure. It can be observed

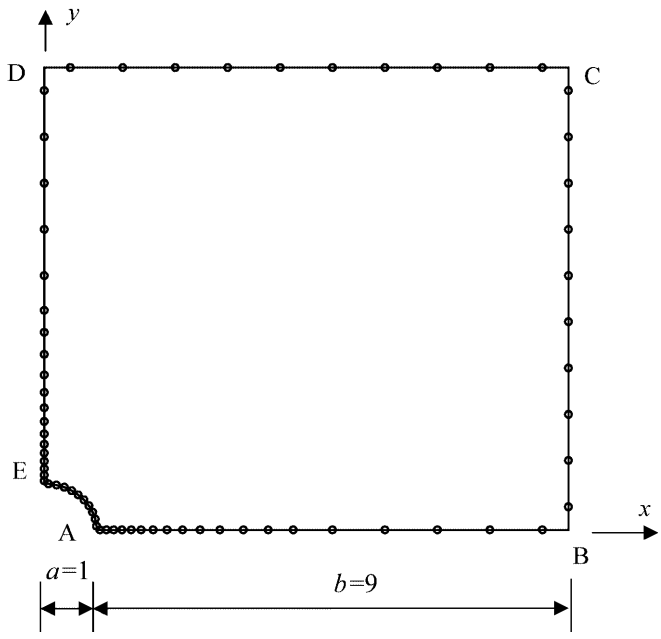

Fig. 6. Nodes in a plate with a central hole subjected to a unidirectional tensile load in the x direction

that the accuracy of the BPIM and BNM is nearly same. Both BPIM and BNM have higher accuracy than that of BEM.

5.2 Plate with a hole

Consider now an infinite plate with a central circular hole subjected to a unidirectional tensile load of 1.0 in the x direction. As a big size finite plate can be considered as a good approximation of the infinite plate, a finite square plate of 20×20 is considered. Taking the advantage of symmetry, only the upper right quadrant of the finite plate is modeled as shown in Fig. 6. Plane strain condition is assumed, and the material properties are $E = 1.0 \times 10^3$, $\nu = 0.3$. Symmetry conditions are imposed on the left and bottom edges, and the inner boundary of the hole is traction free. The tensile load in the x direction is imposed on the right edge. The exact solution for the stresses of infinite plate (Timoshenko and Goodier, 1970) is

$$\sigma_x(x,y) = 1 - \frac{a^2}{r^2}\left\{\frac{3}{2}\cos 2\theta + \cos 4\theta\right\} + \frac{3a^4}{2r^4}\cos 4\theta \tag{19a}$$

$$\sigma_y(x,y) = -\frac{a^2}{r^2}\left\{\frac{1}{2}\cos 2\theta - \cos 4\theta\right\} - \frac{3a^4}{2r^4}\cos 4\theta \tag{19b}$$

$$\sigma_{xy}(x,y) = -\frac{a^2}{r^2}\left\{\frac{1}{2}\sin 2\theta + \sin 4\theta\right\} + \frac{3a^4}{2r^4}\sin 4\theta \tag{19c}$$

where (r, θ) are the polar coordinates with the origin at the centre of the hole, and θ is measured counter-clockwise from the positive x axis.

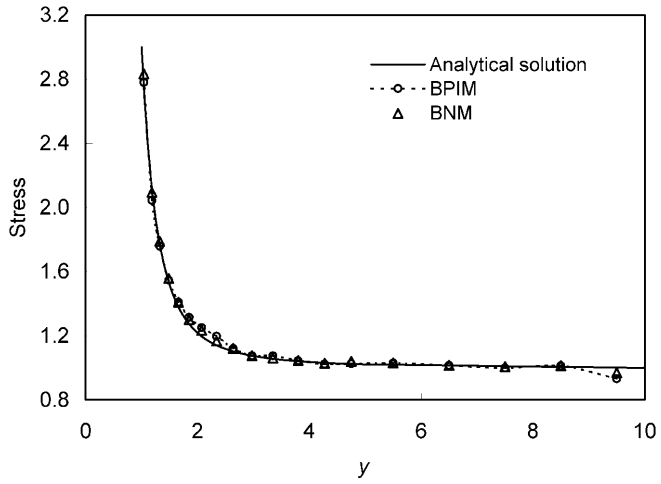

Fig. 7. Stress distribution in a plate with a central hole subjected to unidirectional tensile load (σ_x, at $x = 0$)

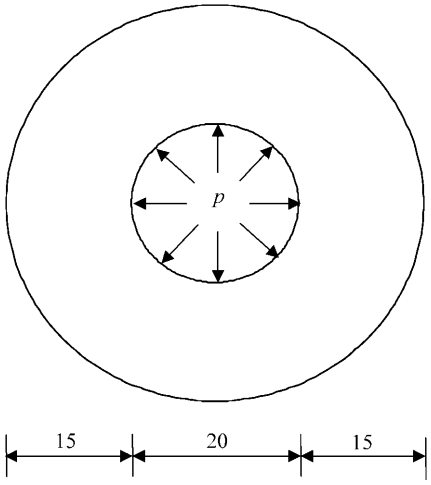

Fig. 8. Hollow cylinder subjected to internal pressure

A total of 68 nodes are used to discretize the boundary (with 10 uniformly distributed nodes on BC, CD and AE, and 19 nonuniformly distributed nodes along AB and DE). The same number integration background cells are used. The influence domain of an evaluation point is determined by Eq. (10) (with $d_{\max} = 2.0$, and the characteristic arc length: $e_i = 1.0$ on AB, BC, CD and DE, $e_i = 0.2$ along AE). If the number of nodes in the influence domain is more than six, only six nodes with shorter arc length to the integration point are used in the interpolation.

As the stress is more critical in the assessment of solution accuracy, detailed results of stress are presented here. The stress σ_x at $x = 0$ obtained by the BPIM is given in Fig. 7 together with the analytical solution for the infinite plate. It can be observed from this figure that the BPIM gives satisfactory results for this problem. The BNM results of this problem are also shown in the same figure for comparison. It is clearly shown that the BPIM and BNM results possess nearly same accuracy for this problem.

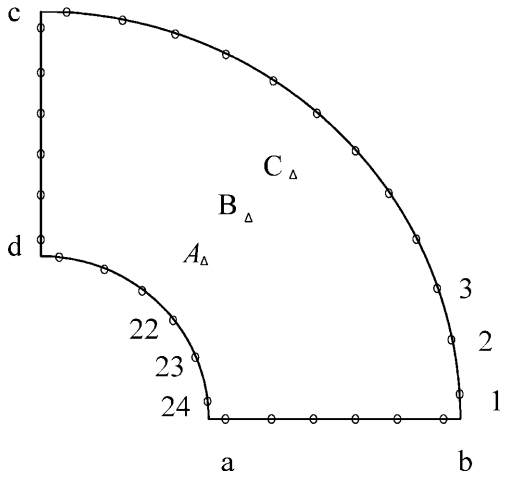

Fig. 9. Arrangement of nodes for the hollow cylinder

5.3
Internal pressurized hollow cylinder

A hollow cylinder under internal pressure is shown in Fig. 8. The parameters are taken as $p = 100$, $G = 8000$, and $v = 0.25$. This problem has been used by several other authors (see, e.g. Brebbia, 1978) as a benchmark problem, as the analytical solution is available. Due to the symmetry of the problem, only one quarter of the cylinder needs to be modeled. As shown in Fig. 9, the boundary of this domain is discretized by 30 nodes (6 uniformly distributed nodes on *ab*, *cd* and *ad*, and 12 uniformly distributed nodes on *bc*). The same number integration background cells are used. Three internal points A, B, and C are selected for examination. The polar coordinates for the three internal points are A(13.75, $\pi/4$), B(17.5, $\pi/4$) and C(21.25, $\pi/4$). The parameter $d_{\max} = 2.0$ is used in Eq. (10) for the influence domains of all evaluation points in the boundary.

The BPIM results are compared to the BNM, conventional BEM and analytical solution. The radial displacements of boundary nodes and internal points are presented in Table 2. The circumferential stresses σ_θ at points A, B and C are listed in the same table. It can be found that the BPIM results are in very good agreement with the analytical solution. In comparison to conventional BEM results, the BPIM solution is, in general, more accurate for the both displacements and stresses.

5.4
A rigid flat punch on a semi-infinite foundation

As BEM type methods have a clear advantage over domain type methods for problems with infinite domain, the BPIM is used to obtain a solution for an indentation produced by a rigid flat punch in a semi-infinite soil foundation, as shown in Fig. 10. In this case, Green's functions for half-plane is employed (Brebbia et al., 1984), and only the contact surface between the punch and half space needs to be discretized.

Consider a rigid punch of length $L = 12$ subjected to a uniform pressure of $p = 100$ on the top. The parameters of the soil foundation are taken as $E = 3.0 \times 10^4$, and $v = 0.3$. The punch is considered to be perfectly smooth,

Table 2. Radial displacement and circumferential stresses for hollow cylinder

Nodes	Exact	BPIM	BNM	BEM
Radial displacements ($\times 10^2$)				
1	0.4464	0.4465	0.4462	0.4468
2	0.4464	0.4478	0.4463	0.4482
3	0.4464	0.4491	0.4498	0.4494
22	0.8036	0.8213	0.8220	0.8266
23	0.8036	0.8214	0.8215	0.8268
24	0.8036	0.8199	0.8223	0.8251
A	0.6230	0.6274	0.6256	0.6319
B	0.5294	0.5342	0.5353	0.5374
C	0.4766	0.4809	0.4826	0.4838
Stress (σ_θ)				
A	82.0113	81.8947	81.8513	82.0192
B	57.9226	58.1285	58.1627	58.1691
C	45.4112	45.6471	45.4597	45.6575

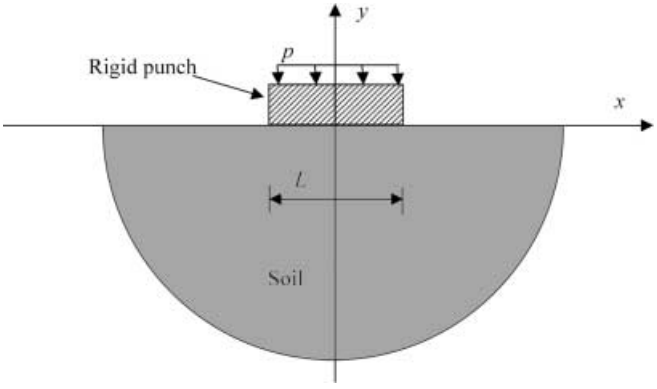

Fig. 10. A rigid punch forced on a semi-infinite soil foundation

and does not result in any fraction force in the interface between the punch and the foundation. An indentation is measured by the vertical displacement of the punch. Plane strain condition is assumed. Due to symmetry, only the right half of the contact surface is discretized by 31 distributed boundary nodes. Thirty one nonuniformly integration background cells are used. Coordinates of these boundary nodes are obtained using the following formula

$$x_m = \frac{6.2(m-1)}{m} \tag{20}$$

where m is the node number, and $m = 1$–31.

The vertical surface displacements of the foundation are assumed to be the same of that of the punch (perfect contact). This assumption is often proven true for rigid punch. A prescribed vertical displacement of the punch is imposed on the contact surface as boundary constraints. The prescribed displacement of the punch can be obtained using the approximate method presented by Poulos and Davis (1974), i.e. the vertical displacement of a vertically loaded rigid area contacted with the rigid punch may be approximated by the mean vertical displacement of a uniformly loaded flexible area of the same shape. The approximation is as follows:

$$v_{\text{rigid}} = 1/2\lfloor v_{\text{center}} + v_{\text{edge}} \rfloor_{\text{flexible}} \tag{21}$$

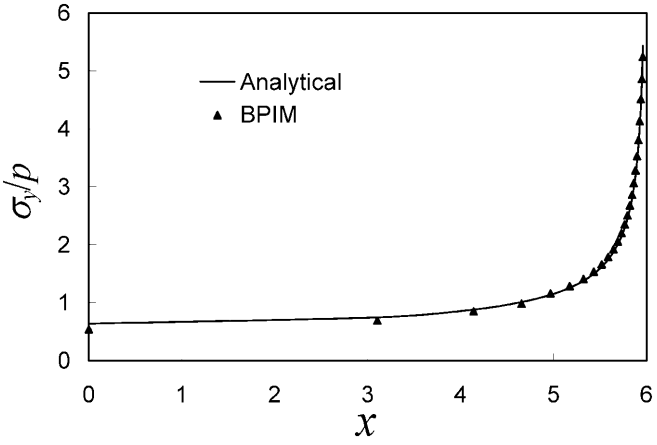

Fig. 11. Contact stresses on the contact surface between the punch and half-space

where v_{rigid} is the vertical displacement of the rigid area contacted with the rigid punch. v_{center} and v_{edge} are vertical displacements at the center and edge, respectively, of the contact area subjected to uniformly loaded, when the contact area is considered as flexible area. The analytical solution of v_{center} and v_{edge} can be obtained in the textbook by Timoshenko and Goodier (1970). The exact solution (Poulos and Davis, 1974) of contact stresses along the contact surface is

$$\frac{\sigma_y}{p} = \frac{2}{\pi}\frac{2}{\sqrt{1-(2x/L)^2}} \tag{22}$$

BPIM is utilized to obtain the contact stresses along the contact surface. The influence domain of an evaluation point is determined by Eq. (10) (with $d_{\max} = 2.0$, and the characteristic arc length: $e_i = 3.0$). If the number of nodes in the influence domain is more than six, only six nodes with shorter arc length to the evaluation point are used in the interpolation. When these six nodes are all sitting in one side of the evaluation point along the boundary, one more node nearest to this evaluation point in the other side is purposely added into the influence domain to avoid the extrapolation.

Figure 11 illustrates the comparison between the contact stresses calculated analytically and by the BPIM along the contact surface. The plot shows an excellent agreement between the analytical and numerical results.

6 Discussion and conclusion

A BPIM is presented for solving 2-D problems of elastostatics. The boundary integral equation is discretized using polynomial point interpolants based on a group of arbitrarily distributed points on the boundary of problem domain. The BPIM does not require any element connectivity in constructing system equation, and possesses the dimensionality advantage. Numerical examples are presented for stress analysis of two-dimensional solids with finite and infinite domain. Compared with the BNM, the present method has following advantages:

- BPIM is computationally much cheaper than BNM due to simpler interpolation scheme and smaller system equation dimension. The number of system equations of BPIM is only a half of that of BNM.
- The imposition of boundary conditions is easy in BPIM due the shape functions have delta property.
- Rigid body movement can be used to avoid some singular integrals.

The present method is very easy to implement, and very flexible for calculating displacements and stresses of desired accuracy in solids. However, the advantages of the methods do not come without some cost. In the point interpolation, the $n = m$ is always satisfied. The influence domain needs to be chosen carefully to obtain a well-conditioned $\mathbf{P}_Q$. In this paper, it is observed that choosing $d_{\max} = 2.0$–3.0 $(n = 3$–$6)$ yields acceptable results.

The BPIM can be extended to 3-D problems to take the full advantages of the meshless concept. However, more research work need be done in utilization BPIM to 3-D problems.

References

Atluri SN, Kim HG, Cho JY (1999) A critical assessment of the truly meshless local Petrov-Galerkin (MLPG), and local boundary integral equation (LBIE) methods. Comput. Mech. 24: 348–372

Atluri SN, Zhu T (1998) A new meshless local Petrov-Galerkin (MLPG) approach in computational mechanics. Comput. Mech. 22: 117–127

Belytschko T, Lu YY, Gu L (1994) Element-free Galerkin methods. Int. J. Numer. Meth. Eng. 37: 229–256

Belytschko T, Organ D (1995) Coupled finite element-element-free Galerkin method. Comput. Mech. 17: 186–195

Brebbia CA (1978) The Boundary Element Method for Engineers. Pentech Press, London; Halstead Press, New York

Brebbia CA, Telles JC, Wrobel LC (1984) Boundary Element Techniques. Springer Verlag, Berlin

Chati MK, Mukherjee S (2000) The boundary node method for three-dimensional problems in potential theory. Int. J. Numer. Meth. Eng. 47: 1523–1547

Chati MK, Mukherjee S, Mukherjee YX (1999) The boundary node method for three-dimensional linear elasticity. Int. J. Numer. Meth. Eng. 46: 1163–1184

Gu YT, Liu GR (2001) A coupled element free Galerkin/boundary element method for stress analysis of two-dimension solid. Comput. Meth. Appl. Mech. Eng. 190: 4405–4419

Hegen D (1996) Element-free Galerkin methods in combination with finite element approaches. Comput. Meth. Appl. Mech. Eng. 135: 143–166

Kothnur VS, Mukherjee S, Mukherjee YX (1999) Two-dimensional linear elasticity by the boundary node method. Int. J. Solids and Struct. 36: 1129–1147

Liu GR (1999) A point assembly method for stress analysis for solid. In: Shim VPW (ed) Impact Response of Materials and Structures, pp 475–480. Oxford, New York

Liu GR, Gu YT (2000) Coupling element free Galerkin and hybrid boundary element methods using modified variational formulation. Comput. Mech. 26: 166–173

Liu GR, Gu YT (2001) A point interpolation method for two-dimensional solid. Int. J. Numer. Meth. Eng. 50: 937–951

Liu GR, Yang KY (1998) A penalty method for enforce essential boundary conditions in element free Galerkin method. The Proceedings of the 3rd HPC Asia'98. Singapore, pp 715–721

Liu WK, Jun S, Zhang YF (1995) Reproducing kernel particle methods. Int. J. Numer. Meth. Eng. 20: 1081–1106

Mukherjee YX, Mukherjee S (1997) Boundary node method for potential problems. Int. J. Num. Meth. Eng. 40: 797–815

Nayroles B, Touzot G, Villon P (1992) Generalizing the finite element method: diffuse approximation and diffuse elements. Comput. Mech. 10: 307–318

Poulos HG, Davis EH (1974) Elastic Solution for Soil and Rock Mechanics. Wiley, London

Timoshenko SP, Goodier JN (1970) Theory of Elasticity, 3rd edn. McGraw-Hill, New York

Wang JG, Liu GR, Wu YG (2001) Several numerical problems in point interpolation methods. submitted

Zhu T, Atluri SN (1998) A modified collocation and a penalty formulation for enforcing the essential boundary conditions in the element free Galerkin method. Comput. Mech. 21: 211–222